Ultrasonics Sonochemistry 107 (2024) 106934

Contents lists available at ScienceDirect

Ultrasonics Sonochemistry

journal homepage: www.elsevier.com/locate/ultson

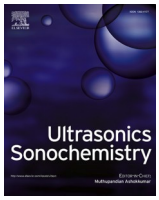

Ultrasound-assisted modification of soybean protein isolate with L-histidine: Relationship between structure and function

Jingwen Xu [a,1], Shizhang Yan [a,1], Jing Xu [b,*], Baokun Qi [a,*]

[a] College of Food Science, Northeast Agricultural University, Harbin, Heilongjiang 150030, China
[b] College of Arts and Sciences, Northeast Agricultural University, Harbin, Heilongjiang 150030, China

ARTICLE INFO

Keywords:
Soybean protein isolate
L-histidine, Ultrasound
Structural characterization
Functional properties

ABSTRACT

Herein, the effects of ultrasound-assisted L-histidine (L-His) on the physicochemical properties and conformation of soybean protein isolate (SPI) were investigated. Particle size, zeta potential, turbidity, and solubility were used to evaluate protein aggregation, and the relationship between structural and functional changes of the proteins was characterized using spectral analysis, surface hydrophobicity, emulsification, and antioxidant properties. After ultrasound-assisted L-His treatment, SPI exhibited a smaller particle size, higher solubility, and more homogeneous micromorphology owing to the decrease in alpha-helix content and subsequent increases in zeta potential and active sulfhydryl content. In addition, spectral analysis showed that L-His and SPI could form a complex, which changed the microenvironment of the amino acid residues in SPI, thus improving its emulsification and antioxidant properties. At the concentration of L-His was 0.3 % w/w, the nanocomplex had a smaller particle size (140.03 nm), higher ζ-potential (–23.63 mV), and higher emulsification stability (22.48 min).

1. Introduction

Soybean protein isolate (SPI) is a high-quality vegetable protein with agricultural sustainability that contains all essential amino acids, thus providing a good amino acid balance [10]. It is considered a substitute for egg white and milk proteins because of its excellent nutritional value and functional activity [15]. SPI comprises 11S (soybean globulin) and 7S (*β*-conglycinin) [20], however, numerous disulfide and hydrogen bonds and non-covalent interactions cause these two globulins to aggregate. This phenomenon results in poor protein conformational flexibility and suboptimal functional properties, thus limiting their application in food systems [35]. Therefore, to promote the high-value utilization of proteins, different modification methods are used to enhance their functional characteristics.

Ultrasound technology is a non-thermal green technology used in various fields of food processing and has a certain effect on protein modification [23]. In liquid–solid systems, cavitation and high shear waves generated via ultrasound can cause the unfolding and partial denaturation of protein molecules. This exposes surface active sites and results in changes to protein structure and aggregation states, which ultimately leads to changes in the functional properties of proteins [25]. While the results of pure ultrasound treatment are closely related to ultrasound conditions, such as power and time, determining the optimal conditions to achieve the best state of modified proteins is challenging. Currently, combining ultrasound with other technologies to modify proteins has attracted increasing attention. For example, Yang et al. [34] reported that an ultrasound-assisted pH shift resulted in structural changes in Perilla isolate proteins and enhanced their emulsification and foaming properties. Additionally, Zhang et al. [36] found that the combined treatment of ultrasound and ionic liquids resulted in structural changes in SPI and improved the emulsification and antioxidant activities of the SPI hydrolysis products. Li et al. [13] comparatively analyzed the effects of ultrasound-assisted glycosylation on the physicochemical and foaming properties of ovotransferrin (OVT) and showed that their synergy improved the interfacial and foaming properties of OVT.

Methods for modifying proteins with basic amino acids are currently under development. L-histidine (L-His), an essential amino acid found in the active sites of proteins, is involved in protein synthesis and plays an important role in human growth, tissue repair, and ulcer treatment [21]. L-His has a unique structural feature with an alkaline imidazole group in its side chain, and the imidazole rings can form complexes with non-

* Corresponding authors.
E-mail addresses: xujing@neau.edu.cn (J. Xu), qibaokun22@163.com (B. Qi).
[1] These authors contributed equally.

https://doi.org/10.1016/j.ultsonch.2024.106934
Received 16 April 2024; Received in revised form 26 May 2024; Accepted 30 May 2024
Available online 31 May 2024

covalent interactions between other molecular structural units and metal ions [3]. For example, Wang et al. [26] reported the effect of L-His on the emulsification properties of soy protein at various ionic concentrations, where the physicochemical changes induced by L-His enhanced the emulsification properties of SPI. Guo et al. [5] investigated the effects of L-His and L-lysine (L-Lys) on the emulsification and interfacial properties of porcine myofibrillar proteins (MPs) and found that L-His and L-Lys enhanced the stability of MP emulsions at low ionic strength by altering the structure and interfacial behavior of the MPs. Therefore, we hypothesized that the ultrasound-assisted L-His modification of SPI is a promising approach to improve its functional properties.

In this study, we modified SPI with L-His using ultrasound and investigated the effect of ultrasound-assisted L-His treatment on the physicochemical properties of SPI using particle size analysis, zeta potential, turbidity, and solubility. Changes in protein sulfhydryl content, secondary structure, spatial conformation, surface hydrophobicity, emulsification, and antioxidant ratings were characterized to determine their effects on protein function.

2. Materials and methods

2.1. Materials

Mature soybeans were harvested in 2023 (variety Nanxiadou 52). L-His, 1-Anilino-8-naphthalenesulfonate (ANS), sodium dodecyl sulfate (SDS), 2,2′-azidobis (3-ethylbenzothiazoline-6-sulfonic acid) (ABTS), 2,2-diphenyl-1-butyrylhydrazine (DPPH), and 5,5′-dithiodinitrobenzoic acid (DTNB) were purchased from Yuanye Bioengineering Co., Ltd. (Shanghai, China). The remaining materials and reagents used in the study were of analytical grade.

2.2. Preparation of SPI

Dissolve 300 g of defatted soybean powder in 3 L of deionized water, stir thoroughly, and adjust the pH of the solution to 9.0 using NaOH (2 M). After sufficient dissolution, centrifuge the solution at 9000 rpm for 30 min and collect the supernatant. Then adjust the pH of the supernatant to 4.5 using HCl solution (2 M), centrifuge the mixed solution (6500 rpm, 20 min), and collect the precipitate. Subsequently, dissolve the precipitate in deionized water and wash it repeatedly three times. After washing, collect the precipitate and finally adjust the solution to pH 7.0 with 2 M NaOH. Collect the supernatant and freeze-dry the protein using a vacuum dryer (Scientz-18 N/a, Scientz, China). The protein content was determined to be 92.02 g/100 g using the Kjeldahl nitrogen method.

2.3. Ultrasonic synergistic l-his processing of SPI

The SPI powder was dispersed in deionized water and stirred uniformly for 3 h at room temperature to make a 10 mg/mL SPI dispersion. The pH of the SPI dispersion was adjusted to 7.0 with 1 M NaOH as a blank control and recorded as untreated SPI. SPI dispersions were sonicated according to the method described by Huang et al. [9]. The SPI dispersions were sonicated at 20 kHz at a power of 400 W for 10 min (pulse duration of 5 s on and 2 s off). To the sonicated SPI solution, 0 %, 0.1 %, 0.2 %, 0.3 %, 0.4 %, and 0.5 % L-His were added, the pH of the mixed solution was adjusted to 7.0 ± 0.1, and the solution was stirred at a stable pH for 1 h. The resulting solution was freeze-dried to obtain sonicated SPI powders with different L-His concentrations, denoted as U-0 %, U-0.1 %, U-0.2 %, U-0.3 %, U-0.4 %, and U-0.5 %.

2.4. Determination of average particle size and ζ-potential

Protein samples were configured at a concentration of 0.5 mg/mL, and then the average particle size and ζ-potential of the protein samples were determined using a Malvern particle sizer (Zetasizer NANO ZS90), with the parameters of the device set at refractive indices of 1.46 and 1.33 for the particles and dispersant, respectively, and an absorption parameter of 0.001.

2.5. Determination of fourier transform infrared spectroscopy

Accurately weigh 2 mg of freeze-dried sample powder, mix with 198 mg of potassium bromide, and thoroughly grind in an agate mortar. Subsequently, the tablet was pressed using a tablet press and placed on an FT-IR spectrometer (FTIR-650, Tianjin Gangdong Biotechnology Co., Ltd., Tianjin, China) for scanning and measurement. The measurement parameters are as follows: scanning speed is 32 times, scanning range is 4000–400 cm^{-1}, and resolution is 4 $cm^{-1.}$

2.6. Determination of circular dichroism

Accurately measure 200 μL of protein solution sample (0.05 mg/mL) and place it in a quartz colorimetric dish. Then, use the Chirascan VX analyzer (Jasco Corp., Tokyo, Japan) to determine the circular dichroism of the sample. The test parameters are set as follows: scanning range 195–260 nm, scanning speed of 100 nm/min, and data interval of 0.5 nm.

2.7. Determination of intrinsic fluorescence spectroscopy

Prepare a protein solution with a concentration of 0.5 mg/mL, accurately weigh 3 mL and place it in a fluorescent colorimetric dish. Use a fluorescence spectrophotometer (930F, Shanghai Yidian Fluorescence Spectrometer, Shanghai, China) to measure the fluorescence spectrum of the sample. The measurement parameters are set as follows: excitation wavelength and emission wavelength are set to 290 nm and 300–500 nm respectively, scanning speed is 2000 nm/min, and slit width is 5 nm.

2.8. Determination of UV–Vis spectroscopy

Prepare a protein solution with a concentration of 0.5 mg/mL, accurately weigh 3 mL of the protein solution and place it in a quartz colorimetric dish. Use a UV–Vis spectrophotometer to measure the UV spectrum of the solution. The measurement parameters are set as follows: slit width of 1.0 nm, scanning range of 200–600 nm, scanning speed of medium, using PBS as the blank control.

2.9. Surface sulfhydryl content measurement

The protein solutions (10 mg/mL) were centrifuged at 5000 rpm for 15 min, and the supernatant was diluted to 1.0 mg/mL with deionized water. Then, 4 mL of the dilution was added to 100 μL of freshly prepared DTNB at a concentration of 10 mM, and the absorbances of the solutions at 412 nm were measured following 15 min of reaction while protected from light. The surface sulfhydryl content was calculated according to Eq. (1):

$$SH\ (\mu mol/g) = A \times 10^6/(\rho \times \varepsilon) \quad (1)$$

where A is the absorbance of the solutions at 412 nm, ε is the extinction coefficient, and ρ is the protein concentration.

2.10. Determination of surface hydrophobicity

Protein solution at a concentration of 1 mg/mL was configured and diluted to different concentrations (0.02–0.1 mg/mL) using deionized water, in addition, ANS solution at a concentration of 8 mM was configured, and then 4 mL of sample solution at different concentrations were mixed with 20 μL of ANS solution respectively and reacted for 30 min away from light. Then, the fluorescence intensity was measured

using an F-600 fluorescence spectrometer. The excitation and emission wavelengths were set at 390 and 470 nm, respectively, and the width of the slit was 5 nm. The surface hydrophobicity was calculated as the slope of the concentration of proteins and their fluorescence intensities.

2.11. Observation of microstructure

The freeze-dried protein powder samples were glued to a sample observatory and the samples were sprayed with gold, and then the microstructure of the samples was observed using a field emission scanning electron microscope (SU8010, German Zeiss), an acceleration voltage of 5 kV, the magnification is 1.5 k times.

2.12. Solubility measurement

A sample was prepared at a concentration of 1.0 mg/mL and centrifuged. The supernatant after centrifugation was mixed with the biuret reagent and reacted for 30 min. The absorbance of the mixed solution at 540 nm was then measured using a UV spectrophotometer. The soluble protein content of the sample was calculated using bovine serum albumin as a standard. Protein solubility was expressed as the percentage of protein content in the supernatant to the total protein in the solution.

2.13. Turbidity measurement

The absorbance at 600 nm was measured as the turbidity of the sample (1.0 mg/mL, 10 mM PBS) using a UV spectrophotometer (V-5800, Shanghai Metash Instruments Co., Ltd, Shanghai, China).

2.14. Emulsifying property measurement

SPI sample solutions (10 mg/mL) were prepared as the aqueous phase and soybean oil as the oil phase with an oil-to-water ratio of 1:9. Each sample was mixed twice for 2 min at 10000 rpm using a high-speed shear homogenizer. From the bottom of the emulsion, 50 μL was aspirated and 5 mL of 0.1 % SDS solution prepared in advance was added. The absorbance of the sample was measured at 500 nm to calculate the emulsification activity index (EAI) according to Eq. (2). The homogenized emulsion rested for 10 min, and the absorbance of the sample was measured in the same manner. The emulsion stability index (ESI) was calculated according to Eq. (3):

$$EAI = \frac{2 \times 2.303 \times 100 \times A_0}{C \times \varphi \times 10000} \tag{2}$$

$$ESI = \frac{A_0 \times 10}{A_0 - A_{10}} \tag{3}$$

where A_0 and A_{10} are the absorbances of the emulsion at 0 and 10 min of standing, respectively; C is the protein concentration in the sample solution (g/mL); and φ is the fraction of oil used to form the emulsion (10 %).

2.15. Antioxidant characteristics

2.15.1. DPPH radical scavenging activity

Briefly, 4 mL of sample or buffer solution (control) was acquired, and 4 mL of DPPH solution with a concentration of 0.01 mM was added, mixed well, and the mixture was placed in the dark at 25 ℃ for 30 min. The absorbance was measured at 517 nm using a UV spectrophotometer, and the DPPH radical scavenging rate was calculated according to Eq. (4):

$$DPPH = \frac{A_s - A_c}{A_b} \times 100\% \tag{4}$$

where A_s, A_c, and A_b are the absorbances of the sample, control, and blank, respectively.

2.15.2. ABTS radical scavenging activity

The ABTS reserve solution was obtained by mixing ABTS solution (7 mM) with an equal volume of potassium persulfate solution (2.45 mM). The mixture was reacted in the dark for 12 to 16 h. Then, 1 mL sample (1 mg/mL) was added to 4 mL ABTS solution (absorbance of 0.70 ± 0.02) and thoroughly mixed. The blank group was substituted with an equal volume of PBS for the sample solution and reacted for 5 min while in the dark. The absorbance was measured at 734 nm, and the ABTS radical scavenging rate was calculated according to Eq. (5):

$$ABTS = \frac{A_0 - A_1}{A_1} \times 100\% \tag{5}$$

where A_1 and A_0 are the absorbances of the ABTS and blank samples, respectively.

2.16. Statistical analysis

All experiments were measured three times, and the results were expressed as mean ± standard deviation. Analysis software (SPSS 26.0) was used for the analysis of variance. Differences were considered significant at $p < 0.05$, and Origin 2024 software was used to create diagrams.

3. Results and discussion

3.1. Particle size and zeta potential analysis

The particle size and polydispersity index (PDI) of proteins can be used to characterize their dispersion in solvents. The effects of ultrasound and L-His on particle size and PDI of the proteins are shown in Fig. 1A. Compared to untreated SPI, sonication resulted in a significantly smaller protein particle size. The ultrasound-induced cavitation effect and physical shear can break the non-covalent bonds between proteins, resulting in the fragmentation of protein particles and reduction of particle size [27]. In addition, adding L-His further reduced the particle size of SPI, which may be due to the ultrasound opening of the protein structure. This opening promoted the interaction between the imidazole group of L-histidine and protein side chain, thereby weakening the force between protein molecules and causing the dissociation of protein aggregates [2,27]. Similarly, Li et al. [14] found that alkaline amino acids enhanced protein solubility and reduced protein particle size by increasing the activation energy of protein aggregation. Moreover, the PDI of the solution showed a tendency to decrease and then increase with the increase of L-His concentration. After adding 0.3 % L-His, the SPI solution exhibited the lowest PDI, which suggests that at low concentrations, L-His can increase pH, change electrostatic interactions, and disrupt hydrophobic interactions. In contrast, at high concentrations, L-His and the proteins may be electrostatically bound. Similar results were reported by [4]. Therefore, the effect of basic amino acids on the aggregation state of myosin is related to their ability to increase the pH and net positive charge.

The zeta potential value of the protein solution reflects the interactions between molecules in the solution. The effects of ultrasound and L-His on the potential of the protein solution are shown in Fig. 1B. Compared to untreated SPI, the observed increase in the potential value of sonicated proteins is because sonication utilizes cavitation to open the protein structure, increases the negative surface charge of proteins, improves the electrostatic repulsion between SPI particles, and disrupts existing SPI aggregates, which in turn increases the stability of the protein dispersion [31]. Furthermore, the addition of L-His resulted in a trend of first increasing and then decreasing the potential of the protein solution, which is explained by the same reasoning as that for the change

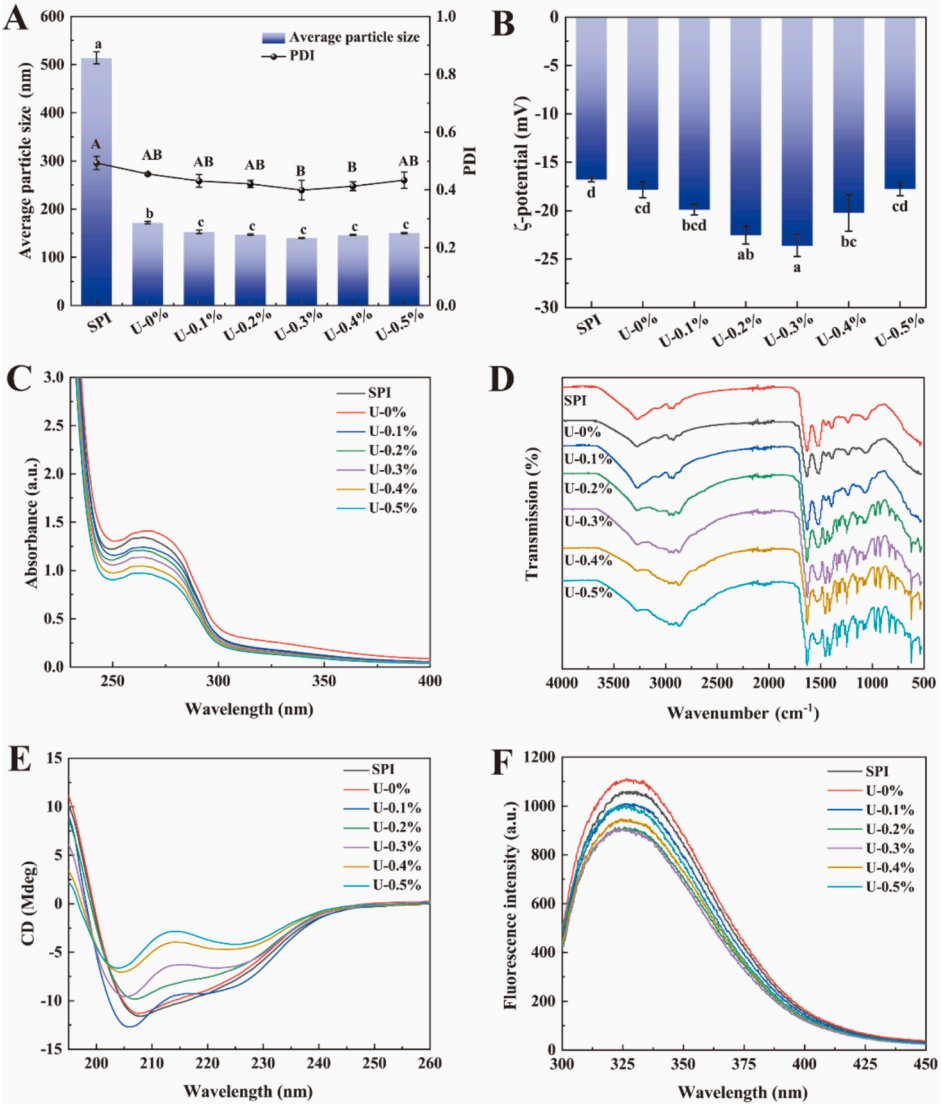

Fig. 1. Average particle size and PDI (A), zeta potential (B), and UV–Vis (C), FT-IR (D), Circular dichroism (E), and fluorescence spectra (F) of SPI treated with ultrasonography in collaboration with L-His.

in particle size. The addition of L-His can increase the pH of the solution, resulting in a higher negative electronegativity for the proteins. When L-His is at a high concentration, it may electrically bind to the proteins, which decreases the value of the protein solution potential [27].

3.2. UV spectral analysis

UV–Vis spectroscopy can be used to assess changes in protein structure, which include conformational and hydration changes, dissociation, or denaturation [29]. The effects of sonication and L-His on the UV absorption of amino acids by proteins are shown in Fig. 1C. SPI exhibited a typical absorption peak at approximately 280 nm, which was attributed to the absorption of tyrosine (Tyr), tryptophan (Trp), and phenylalanine (Phe) in the protein [32]. Compared to untreated SPI, sonication significantly enhanced the absorption peaks in the UV–vis spectrum of SPI, and the maximum absorption wavelength was significantly red shifted. This result was attributed to the cavitation effect and mechanical shear generated by sonication, which resulted in the exposure of hidden hydrophobic groups inside the protein to the solvent environment [31]. However, the fluorescence intensity of the SPI treated with ultrasound synergistically with L-His decreased sequentially with increasing L-His concentration. This result may be attributed to the interaction of L-His with the side chains of the proteins, which masked the UV absorption of the aromatic amino acids in the proteins, resulting in a decrease in UV absorption. Similar findings were found by Wu et al. [27]. Therefore, the incorporation of L-His resulted in the aromatic amino acid groups in MPs being in a more hydrophobic environment.

3.3. FT-IR spectroscopy analysis

The effect of ultrasound on the structure of SPI and interaction between L-His and protein were evaluated using FT-IR spectroscopy, as shown in Fig. 1D. SPI showed four characteristic peaks, including 1631.97 (amide I, C = O stretching), 1516.26 (amine II, N–H bending), 1238.82 (amino III, C–N stretching and N–H deformation), 3278.39 (amide A, hydrogen bond N–H stretching), and 2928.86 cm^{-1} (C–H symmetric stretching) [28]. Compared to untreated SPI, sonication did not significantly improve the amide I and II bands of the protein. This result suggests that sonication had less effect on the secondary structure of the protein, which is consistent with the results of the CD analysis in this study [8]. However, sonication resulted in a significant blue shift (3267.33 cm^{-1}) of the amide A band of the protein, which may be related to the increase in intramolecular β-sheet interactions and

breaking of hydrogen bonds [31]. In addition, adding L-His significantly enhanced the peak intensities of the amide I, II, and A bands of the protein, and a new characteristic peak appeared at 1270 cm^{-1}, which may be attributed to the interaction between the imidazolyl group contained in L-His and side chain of the protein, resulting in the stretching vibration of the C–H/N–H bond [18].

3.4. CD analysis

The CD spectra of the SPI samples obtained using sonication and L-His are shown in Fig. 1E. All samples showed significant negative peaks at approximately 208 and 225 nm and a positive peak at 195 nm, which corresponds to the typical peaks of α-helices and β-sheets of proteins [30]. The combination of ultrasound and L-His treatment resulted in a change in the ellipticity of the CD of the proteins compared to untreated SPI, suggesting that their secondary structure was significantly altered. However, ultrasound treatment without L-His did not change the ellipticity, suggesting that ultrasound does not affect its secondary structure [22]. Similar results were reported by Hu et al. [7], who showed that sonication failed to significantly disrupt the hydrogen bonds between the C = O and H–N groups in the polypeptide backbone. Cavitation shearing may disrupt the tertiary structure but leaves most of the secondary structure elements intact. The secondary structure contents of all samples are summarized in Table 1. For ultrasound-treated proteins, sonication had no effect on the ellipticity of the proteins; thus, their secondary structure remained unchanged ($p > 0.05$). For SPI treated with ultrasound synergistically with L-His, the α-helix content of the proteins was significantly reduced, suggesting that adding L-His disrupts the hydrogen bonds that stabilize α-helices and causes a rearrangement of the polypeptide chains [6,27]. In general, α-helices are ordered secondary structures of protein molecules. Thus, L-His inhibits the aggregation of protein molecules by inducing the absence of ordered secondary structures, which is attributed to the presence of nucleophilic centers in the imidazole ring that may disrupt these hydrogen bonds, thereby affecting their structure [2].

3.5. Intrinsic fluorescence spectroscopy analysis

The intrinsic fluorescence of proteins originates from amino acid residues with aromatic groups within the protein molecule and can be used to characterize tertiary structural changes in proteins. The effects of sonication and L-His on the internal fluorescence of SPI are shown in Fig. 1F. Compared to untreated SPI, the fluorescence intensity of SPI significantly increased after sonication, because ultrasound causes the three-dimensional conformation of the protein to become stretched, thus prompting the exposure of internal hidden chromophores [31]. Notably, the addition of L-His had a different effect on the fluorescence intensity of the protein. When the concentration of L-His was < 0.3 %, the fluorescence intensity decreased as the concentration of L-His increased. This result could be attributed to the interaction of L-His with the aromatic amino acids of the protein, thus masking its chromophore. In contrast, when the concentration of L-His continued to increase, the fluorescence intensity of the protein increased but remained lower than that of the original SPI. The imidazole ring contained in L-His binds to the charged residues of the protein via electrostatic effects at high concentrations, destroying the intramolecular and intermolecular ionic bonding and thus altering the protein structure [2].

Table 1
Secondary structure contents of SPI treated with ultrasound in collaboration with L-His.

Sample	α-helix	β-sheet	β-turn	Random coil
SPI	13.6	33.2	20.0	33.4
U-0 %	13.7	33.4	20.0	33.2
U-0.1 %	13.6	31.6	21.1	33.8
U-0.2 %	12.3	35.4	20.1	33.3
U-0.3 %	11.5	35.7	20.7	33.6
U-0.4 %	9.8	39.2	20.2	33.5
U-0.5 %	9.3	40.2	20.3	33.5

3.6. Surface sulfhydryl group content

Changes in the free sulfhydryl content of proteins can be used to assess alterations in protein conformation. The effects of sonication and L-His treatment on the sulfhydryl content of proteins are shown in Fig. 2A. Sonication resulted in a significant increase in the sulfhydryl content of proteins compared to untreated SPI, which was attributed to the cavitation effect and mechanical shear generated by sonication. This phenomenon resulted in conformational stretching of the proteins, thus exposing their internal sulfhydryl moieties [33]. In addition, adding L-His further increased the sulfhydryl content of proteins, whereas it decreased when the concentration of L-His exceeded 0.3 %. This result may be attributed to the following reasons. At low concentrations, as the concentration of L-His increased, it could interact with amino acid residues in proteins via cation–π, π–π stacking, hydrogen–π, and hydrogen bonding interactions, thus making the protein structure stretch and exposing its internal sulfhydryl groups [16]. When the concentration continued to increase, L-His might have electrostatic interactions with the protein, resulting in the formation of microaggregates that mask the internal sulfhydryl groups. This result is consistent with the PDI results, and similar results have been reported by Lei et al. [12]. Therefore, basic amino acids can induce conformational changes in proteins, thereby altering the exposed sulfhydryl content.

3.7. Surface hydrophobicity analysis

The surface hydrophobicity index indicates the number of hydrophobic groups exposed on the surface of a protein, which not only reflects the conformation of the protein but is also closely related to certain functional properties (e.g., solubility and emulsification) [31]. The effects of the synergistic action of ultrasound and L-His on the surface hydrophobicity of SPI are shown in Fig. 2B. Compared to untreated SPI, ultrasound treatment significantly increased the surface hydrophobicity of SPI owing to the cavitation effect of ultrasound on protein macromolecules. This effect instantaneously generated strong turbulence and high-energy shear waves, changed the protein structure, and induced the exposure of hydrophobic groups, thus increasing surface hydrophobicity [8]. However, after adding L-His, the surface hydrophobicity of the protein showed a tendency to decrease and then increase, which may be attributed to two reasons. At low concentrations, L-His may alter the electrostatic properties of myosin via electrostatic binding to exposed negatively charged amino acid residues, which may dislocate hydrophobic surfaces and weaken hydrophobic interactions [4]. In addition, the imidazole ring of L-His can interact with the hydrophobic regions of the protein, shielding them and resulting in a less hydrophobic surface [21]. Similar results were found by Wang et al. [26], who showed that L-His can interact with amino acid residues in proteins via cationic–π, π–π stacking, hydrogen–π, and hydrogen bonding interactions, which resulted in a decrease in the surface hydrophobicity of the protein. In contrast, the surface hydrophobicity of the protein was slightly elevated when the concentration of L-His consistently increased, which may be due to electrostatic interactions between L-His and the protein, thus facilitating the binding of the ANS (anionic probe) to the protein [1].

3.8. Micromorphological analysis

The micromorphologies of the SPI treated in different ways are shown in Fig. 3. For the untreated SPI, the microscopic morphology showed a smooth, large lamellar structure, and after sonication, the intact lamellae of the proteins ruptured and became fragmented due to the mechanical shear force generated by ultrasound [9]. After adding L-

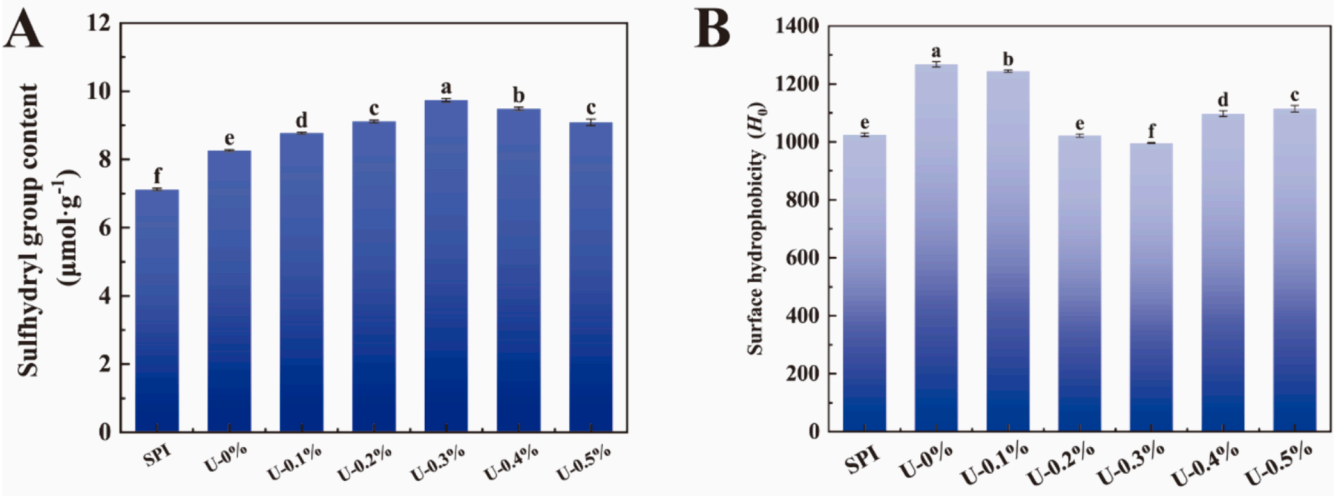

Fig. 2. Sulfhydryl group content (A) and surface hydrophobicity (B) of SPI treated with ultrasonography in collaboration with L-His.

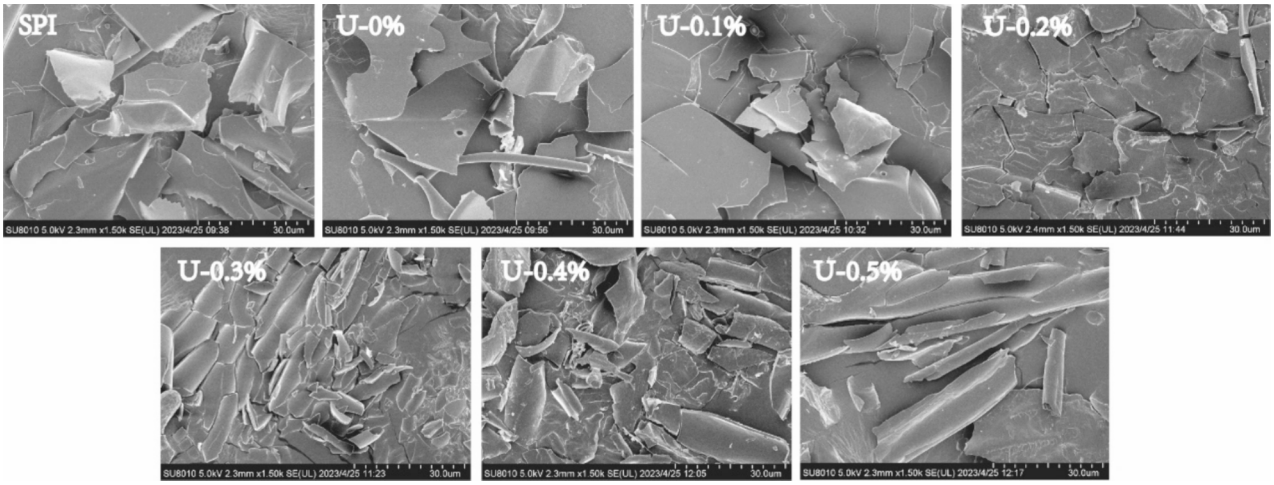

Fig. 3. Scanning electron microscope image of the L-His ultrasonic SPI complex.

His, the micromorphology of the proteins gradually became fragmented with the concentration of L-His, which was most significant at a concentration of 0.3 %. Adding L-His may have altered the secondary structure and three-dimensional conformation of the proteins. Previous studies have shown that changes in protein micromorphology are closely related to changes in protein structure [11]. At concentrations > 0.3 %, the proteins appeared as long-striated structures with relative integrity, which may be due to electrostatic interactions between L-His and the proteins at high concentrations, resulting in microaggregation.

3.9. Solubility and turbidity analysis

Solubility is an important indicator of protein denaturation and aggregation and affects several important functional properties [31]. The effect of ultrasound and L-His on protein solubility is shown in Fig. 4A, where ultrasound significantly increases the solubility of SPI compared to that for untreated SPI. This result may be attributed to the numerous cavitation bubbles and mechanical shear generated during ultrasound treatment, which resulted in the stretching of the protein structure. The change in protein conformation enhanced the interaction of the protein with water, and its solubility increased [8,9]. After adding L-His, the solubility of SPI following ultrasound-assisted treatment first increased and then decreased with additional L-His, reaching the highest solubility with the addition of 0.3 % L-His. This may be due to the interactions between L-His and the proteins, in which the L-His attached to the amino acid side chains and peptide bonds of the proteins, which decreased the electrostatic and hydrophobic interactions [26]. Similar results were found by Wu et al. [27], who showed that after opening the structure of the protein, ultrasound helped the imidazole group of L-His attack its side chains and prevented it from self-aggregating, thus increasing protein solubility. However, the solubility of the proteins did not continue to increase as the concentration of L-His increased, which may be caused by the electrostatic binding of L-His to the proteins at high concentrations, consistent with our results for particle size and PDI.

Turbidity indicates the degree of protein aggregation in solution [31]. The effects of ultrasound and L-His on SPI turbidity is shown in Fig. 4B. Sonication reduces the turbidity of SPI compared to that for untreated SPI, which is attributed to the fact that ultrasound disrupts protein–protein interactions and facilitates protein–water interactions with increased solubility and smaller particle sizes [9]. The turbidity of the samples treated with ultrasound synergistically with L-His showed different trends, and reached a minimum when the concentration of L-His was 0.3 %. Thus, L-His may bind to amino acid residues in the proteins exposed by ultrasound induction and disrupt the electrostatic interactions between the protein molecules, which may reduce the aggregation of proteins and result in decreased particle size and turbidity [4,27]. However, when the concentration of L-His continued to increase, the turbidity of the protein solution showed an increasing trend, which

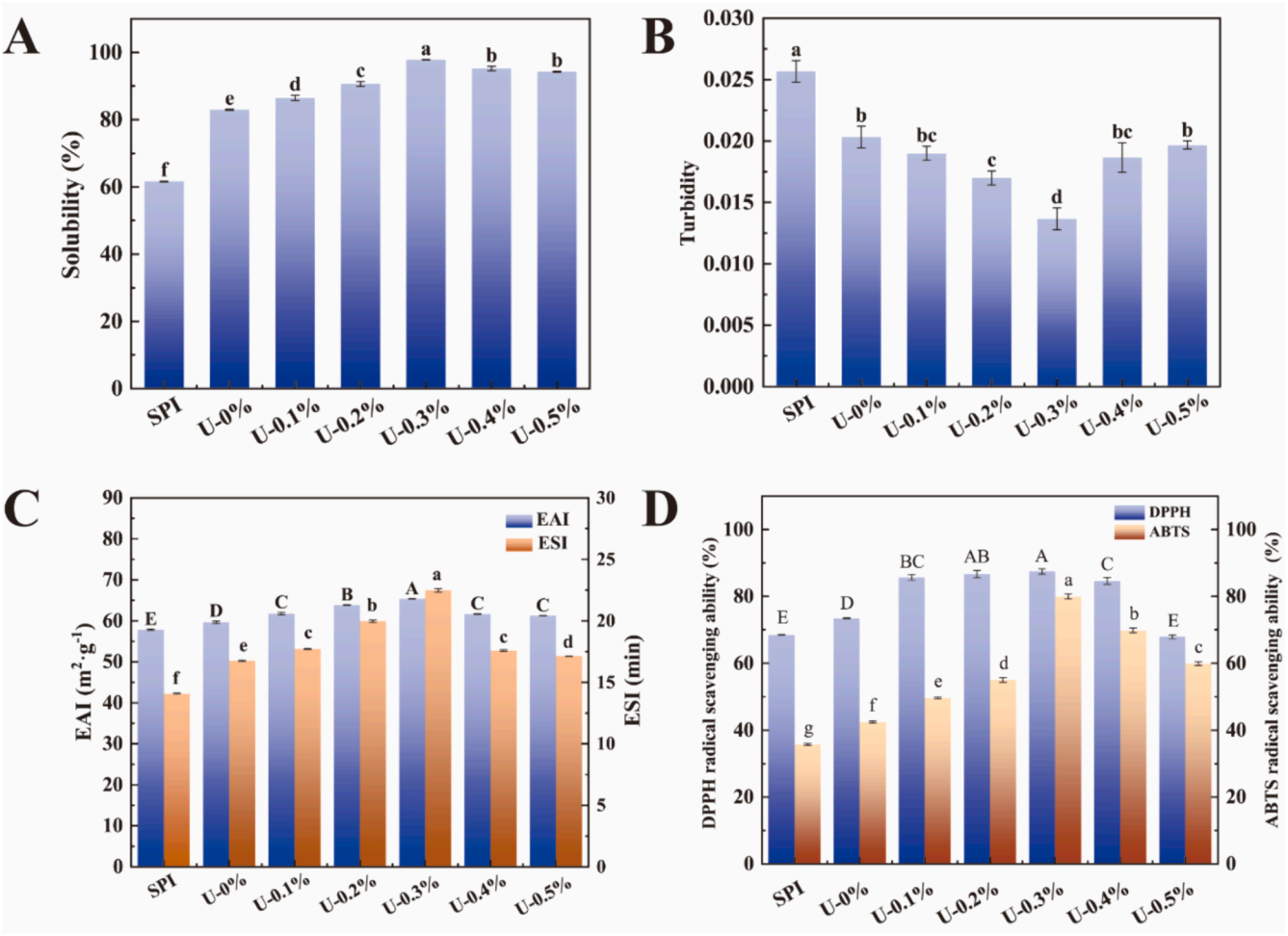

Fig. 4. Solubility (A), turbidity (B), and emulsifying (C) and antioxidant properties (D) of SPI treated with ultrasound in collaboration with L-His.

may be due to electrostatic interactions between excess histidine and the proteins, resulting in the formation of microaggregates.

3.10. Analysis of emulsification characteristics

The EAI is the ability of proteins to form an interfacial layer at the oil–water interface, and the ESI is the ability of an emulsion stabilized by an emulsifier to produce droplets that resist strain [33]. The effect of ultrasonic treatment with L-His on the emulsification properties of SPI is shown in Fig. 4C. Compared to untreated SPI, ultrasound significantly improved the emulsification properties of SPI, which may be attributed to the cavitation effect and mechanical shear generated by the ultrasound treatment. This caused the conformations in SPI to become stretched, thus exposing more hydrophobic amino acid side chains and promoting the adsorption of proteins to form an interfacial membrane at the oil–water interface [31,33]. Similar results have been reported by Sha et al. [19]. Therefore, the ultrasonic treatment induced a faster adsorption of proteins at the oil–water interface, improved emulsification, and enhanced the physical stability of the emulsion. The addition of L-His further increased the emulsification properties of SPI, which may be related to an increase in SPI solubility and decrease in surface hydrophobicity [26]. In addition, L-His may affect the interfacial behavior of SPI by balancing the interfacial tension, which results in the formation of a denser interfacial film that prevents the aggregation of droplets in O/W emulsions, thus improving the emulsification properties of the protein [5,37]. However, the EAI and ESI of the proteins decreased when the concentration of L-His was continuously increased, which might be due to the aggregation of SPI caused by excess L-His. Thus, the proteins were adsorbed with a large spatial site resistance, resulting in an unstable interfacial membrane.

3.11. Analysis of antioxidant properties

The DPPH and ABTS radical scavenging rates were used to determine the antioxidant properties of SPI under synergistic ultrasound and L-His treatment, and the results are shown in Fig. 4D. The untreated SPI presented a superior radical scavenging rate, which might have been caused by the binding of amino acids exposed on the outer surface of the protein to free radicals [17,30]. Compared to untreated SPI, SPI treated with ultrasound significantly improved the antioxidant properties by modifying and unfolding the protein structure, which resulted in the exposure of antioxidant amino acids within the protein [8]. In addition, adding L-His further enhanced the antioxidant properties of the protein, which were highest when the L-His concentration was 0.3 %. L-His scavenges hydroxyl radicals and singlet oxygen and can directly interact with free radicals and carbonyl proteins for antioxidant protection [24]. However, when the concentration of L-His was continuously increased, the antioxidant property of the protein was weakened, but remained higher than that of SPI alone. This result could be attributed to the electrostatic interactions of L-His with the protein, which reduces the solubility (Fig. 4A) of the complex and inhibits its binding to free radicals.

4. Conclusion

Herein, we investigated ultrasound-assisted L-His-modification of

SPI. The combination of ultrasound and L-His treatment effectively improved the functional properties of SPI by altering its conformation. Ultrasound combined with L-His treatment at appropriate concentrations decreased the mean particle size, turbidity, and surface hydrophobicity and increased the absolute value of the zeta potential, solubility, and surface sulfhydryl content of SPI. In addition, spectral analysis showed that ultrasound-assisted L-His altered the secondary structure and three-dimensional conformation of SPI. The α-helix content of SPI gradually decreased with increasing L-His concentration, and the microenvironment of the hydrophobic amino acids in the protein was changed. When L-His content was 0.3 %, the proteins exhibited optimal emulsification and antioxidant properties. Therefore, ultrasound combined with L-His treatment can effectively alter the structure of SPI and improve its functional properties. The combination of ultrasound and alkaline amino acid treatments has potential applications in soy protein processing and utilization.

CRediT authorship contribution statement

Jingwen Xu: Writing – original draft. **Shizhang Yan:** Software, Formal analysis. **Jing Xu:** Supervision, Formal analysis. **Baokun Qi:** Writing – review & editing, Funding acquisition.

Declaration of competing interest

The authors declare that they have no known competing financial interests or personal relationships that could have appeared to influence the work reported in this paper.

Acknowledgments

We gratefully acknowledge the financial support received from the National Soybean Industrial Technology System of China (CARS-04-PS32).

References

[1] T. Arakawa, D. Ejima, K. Tsumoto, N. Obeyama, Y. Tanaka, Y. Kita, S.N. Timasheff, Suppression of protein interactions by arginine: A proposed mechanism of the arginine effects, Biophys. Chem. 127 (1–2) (2007) 1–8, https://doi.org/10.1016/j.bpc.2006.12.007.

[2] X. Chen, Y. Zou, M. Han, L. Pan, T. Xing, X. Xu, G. Zhou, Solubilisation of myosin in a solution of low ionic strength l -histidine: significance of the imidazole ring, Food Chem. 196 (2016) 42–49, https://doi.org/10.1016/j.foodchem.2015.09.039.

[3] Y. Chen, K. Tao, W. Ji, V.B. Kumar, S. Rencus-Lazar, E. Gazit, Histidine as a key modulator of molecular self-assembly: peptide-based supramolecular materials inspired by biological systems, Mater. Today 60 (2022) 106–127, https://doi.org/10.1016/j.mattod.2022.08.011.

[4] R. Gao, T. Shi, Q. Sun, X. Li, D.J. McClements, L. Yuan, Effects of l-arginine and l-histidine on heat-induced aggregation of fish myosin: bighead carp (Aristichthys nobilis), Food Chem. 295 (2019) 320–326, https://doi.org/10.1016/j.foodchem.2019.05.095.

[5] X. Guo, F. Gao, Y. Zhang, Z. Peng, M.A. Jamali, Effect of l-histidine and l-lysine on the properties of oil-in-water emulsions stabilized by porcine myofibrillar proteins at low/high ionic strength, LWT 141 (2021) 110883, https://doi.org/10.1016/j.lwt.2021.110883.

[6] X.Y. Guo, Z.Q. Peng, Y.W. Zhang, B. Liu, Y.Q. Cui, The solubility and conformational characteristics of porcine myosin as affected by the presence of l-lysine and l-histidine, Food Chem. 170 (2015) 212–217, https://doi.org/10.1016/j.foodchem.2014.08.045.

[7] H. Hu, I.W.Y. Cheung, S. Pan, E.C.Y. Li-Chan, Effect of high intensity ultrasound on physicochemical and functional properties of aggregated soybean β-conglycinin and glycinin, Food Hydrocoll. 45 (2015) 102–110, https://doi.org/10.1016/j.foodhyd.2014.11.004.

[8] H. Hu, J. Wu, E.C.Y. Li-Chan, L. Zhu, Xu. Zhang, X. Xu, G. Fan, L. Wang, X. Huang, S. Pan, Effects of ultrasound on structural and physical properties of soy protein isolate (SPI) dispersions, Food Hydrocoll. 30 (2) (2013) 647–655, https://doi.org/10.1016/j.foodhyd.2012.08.001.

[9] L. Huang, X. Ding, Y. Li, H. Ma, The aggregation, structures and emulsifying properties of soybean protein isolate induced by ultrasound and acid, Food Chem. 279 (2019) 114–119, https://doi.org/10.1016/j.foodchem.2018.11.147.

[10] F. Ji, J. Xu, Y. Ouyang, D. Mu, X. Li, S. Luo, Y. Shen, Z. Zheng, Effects of NaCl concentration and temperature on fibrillation, structure, and functional properties of soy protein isolate fibril dispersions, LWT 149 (2021) 111862, https://doi.org/10.1016/j.lwt.2021.111862.

[11] Y. Jia, X. Yan, X. Li, S. Zhang, Y. Huang, D. Zhang, Y. Li, B. Qi, Soy protein–phlorizin conjugate prepared by tyrosinase catalysis: Identification of covalent binding sites and alterations in protein structure and functionality, Food Chem. 404 (2023) 134610, https://doi.org/10.1016/j.foodchem.2022.134610.

[12] Z. Lei, Y. Fu, P. Xu, Y. Zheng, C. Zhou, Effects of l -arginine on the physicochemical and gel properties of chicken actomyosin, Int. J. Biol. Macromol. 92 (2016) 1258–1265, https://doi.org/10.1016/j.ijbiomac.2016.08.040.

[13] S. Li, S. Zhang, Y. Liu, X. Fu, X. Xiang, S. Gao, Effects of ultrasound-assisted glycosylation on the interface and foaming characteristics of ovotransferrin, Ultrason. Sonochem. 84 (2022) 105958, https://doi.org/10.1016/j.ultsonch.2022.105958.

[14] S. Li, Y. Zheng, P. Xu, X. Zhu, C. Zhou, l-Lysine and l-arginine inhibit myosin aggregation and interact with acidic amino acid residues of myosin: the role in increasing myosin solubility, Food Chem. 242 (2018) 22–28, https://doi.org/10.1016/j.foodchem.2017.09.033.

[15] G. Liang, W. Chen, X. Qie, M. Zeng, F. Qin, Z. He, J. Chen, Modification of soy protein isolates using combined pre-heat treatment and controlled enzymatic hydrolysis for improving foaming properties, Food Hydrocoll. 105 (2020) 105764, https://doi.org/10.1016/j.foodhyd.2020.105764.

[16] S.-M. Liao, Q.-S. Du, J.-Z. Meng, Z.-W. Pang, R.-B. Huang, The multiple roles of histidine in protein interactions, Chem. Cent. J. 7 (1) (2013) 44, https://doi.org/10.1186/1752-153X-7-44.

[17] D.J. McClements, C.E. Gumus, Natural emulsifiers — biosurfactants, phospholipids, biopolymers, and colloidal particles: molecular and physicochemical basis of functional performance, Adv. Colloid Interface Sci. 234 (2016) 3–26, https://doi.org/10.1016/j.cis.2016.03.002.

[18] A.M. Petrosyan, Vibrational spectra of l-histidine perchlorate and l-histidine tetrafluoroborate, Vib. Spectrosc 43 (2) (2007) 284–289, https://doi.org/10.1016/j.vibspec.2006.03.001.

[19] L. Sha, A.O. Koosis, Q. Wang, A.D. True, Y.L. Xiong, Interfacial dilatational and emulsifying properties of ultrasound-treated pea protein, Food Chem. 350 (2021) 129271, https://doi.org/10.1016/j.foodchem.2021.129271.

[20] H. Sharafodin, N. Soltanizadeh, Potential application of DBD plasma technique for modifying structural and physicochemical properties of Soy Protein Isolate, Food Hydrocoll. 122 (2022) 107077, https://doi.org/10.1016/j.foodhyd.2021.107077.

[21] H. Shi, I. Ali Khan, R. Zhang, Y. Zou, W. Xu, D. Wang, Evaluation of ultrasound-assisted L-histidine marination on beef M. semitendinosus: Insight into meat quality and actomyosin properties, Ultrason. Sonochem. 85 (2022) 105987, https://doi.org/10.1016/j.ultsonch.2022.105987.

[22] P.B. Stathopulos, G.A. Scholz, Y.-M. Hwang, J.A.O. Rumfeldt, J.R. Lepock, E. M. Meiering, Sonication of proteins causes formation of aggregates that resemble amyloid, Protein Sci. 13 (11) (2008) 3017–3027, https://doi.org/10.1110/ps.04831804.

[23] R. Tian, J. Feng, G. Huang, B. Tian, Y. Zhang, L. Jiang, X. Sui, Ultrasound driven conformational and physicochemical changes of soy protein hydrolysates, Ultrason. Sonochem. 68 (2020) 105202, https://doi.org/10.1016/j.ultsonch.2020.105202.

[24] A.M. Wade, H.N. Tucker, Antioxidant characteristics of L-histidine, J. Nutr. Biochem. 9 (6) (1998) 308–315, https://doi.org/10.1016/S0955-2863(98)00022-9.

[25] J. Wang, X. Na, W.B. Navicha, C. Wen, W. Ma, X. Xu, C. Wu, M. Du, Concentration-dependent improvement of gelling ability of soy proteins by preheating or ultrasound treatment, LWT 134 (2020) 110170, https://doi.org/10.1016/j.lwt.2020.110170.

[26] Y. Wang, T. Ma, C. Liu, F. Guo, J. Zhao, L-Histidine improves solubility and emulsifying properties of soy proteins under various ionic strengths, LWT 152 (2021) 112382, https://doi.org/10.1016/j.lwt.2021.112382.

[27] W. Wu, Q. Jiang, P. Gao, D. Yu, P. Yu, W. Xia, L-histidine-assisted ultrasound improved physicochemical properties of myofibrillar proteins under reduced-salt condition—investigation of underlying mechanisms, Int. J. Biol. Macromol. 253 (2023) 126820, https://doi.org/10.1016/j.ijbiomac.2023.126820.

[28] S. Yan, Q. Wang, Y. Li, B. Qi, Gallic acid-functionalized soy protein-based multiple cross-linked hydrogel: mechanism analysis, physicochemical properties, and digestive characteristics, Food Chem. 433 (2024) 137290, https://doi.org/10.1016/j.foodchem.2023.137290.

[29] S. Yan, Q. Wang, J. Yu, Y. Li, B. Qi, Ultrasound-assisted preparation of protein–polyphenol conjugates and their structural and functional characteristics, Ultrason. Sonochem. 106645 (2023), https://doi.org/10.1016/j.ultsonch.2023.106645.

[30] S. Yan, Q. Wang, S. Zhang, Y. Huang, H. Zhu, B. Qi, Y. Li, Oxidized dextran improves the stability and effectively controls the release of curcumin loaded in soybean protein nanocomplexes, Food Chem. 431 (2024) 137089, https://doi.org/10.1016/j.foodchem.2023.137089.

[31] S. Yan, J. Xu, S. Zhang, Y. Li, Effects of flexibility and surface hydrophobicity on emulsifying properties: ultrasound-treated soybean protein isolate, LWT 142 (2021) 110881, https://doi.org/10.1016/j.lwt.2021.110881.

[32] S. Yan, Y. Yao, X. Xie, S. Zhang, Y. Huang, H. Zhu, Y. Li, B. Qi, Comparison of the physical stabilities and oxidation of lipids and proteins in natural and polyphenol-modified soybean protein isolate-stabilized emulsions, Food Res. Int. 162 (2022) 112066, https://doi.org/10.1016/j.foodres.2022.112066.

[33] X. Yan, Y. Jia, H. Man, S. Sun, Y. Huang, B. Qi, Y. Li, Tracking the driving forces for the unfolding and folding of kidney bean protein isolates: revealing mechanisms of dynamic changes in structure and function, Food Chem. 402 (2023) 134230, https://doi.org/10.1016/j.foodchem.2022.134230.

[34] J. Yang, Y. Duan, F. Geng, C. Cheng, L. Wang, J. Ye, H. Zhang, D. Peng, Q. Deng, Ultrasonic-assisted pH shift-induced interfacial remodeling for enhancing the

emulsifying and foaming properties of perilla protein isolate, Ultrason. Sonochem. 89 (2022) 106108, https://doi.org/10.1016/j.ultsonch.2022.106108.
[35] W. Zhang, I.D. Boateng, W. Zhang, S. Jia, T. Wang, L. Huang, Effect of ultrasound-assisted ionic liquid pretreatment on the structure and interfacial properties of soy protein isolate, Process Biochem. 115 (2022) 160–168, https://doi.org/10.1016/j.procbio.2022.02.015.
[36] W. Zhang, L. Huang, W. Chen, J. Wang, S. Wang, Influence of ultrasound-assisted ionic liquid pretreatments on the functional properties of soy protein hydrolysates, Ultrason. Sonochem. 73 (2021) 105546, https://doi.org/10.1016/j.ultsonch.2021.105546.
[37] X. Zhu, L. Li, S. Li, C. Ning, C. Zhou, L-Arginine/l–lysine improves emulsion stability of chicken sausage by increasing electrostatic repulsion of emulsion droplet and decreasing the interfacial tension of soybean oil-water, Food Hydrocoll. 89 (2019) 492–502, https://doi.org/10.1016/j.foodhyd.2018.11.021.